LA-UR- 12-01408

Approved for public release;
distribution is unlimited.

Title: Full-scale fatigue tests of CX-100 wind turbine blades. Part I - testing

Author(s): Stuart G. Taylor *,**
Kevin M. Farinholt*
Gyuhae Park*
Curtt M. Ammerman*

* Los Alamos National Laboratory, Los Alamos, NM
** University of California, San Diego, La Jolla, CA

Intended for: Proceedings of the SPIE Smart Structures/NDE Conference
San Diego, CA, USA
March 11-15, 2012

Form 836 (7/06)

Full-scale fatigue tests of CX-100 wind turbine blades. Part I – testing

Kevin M. Farinholt[a], Stuart G. Taylor*[a,b], Gyuhae Park[a], Curtt M. Ammerman[a]
[a] Los Alamos National Laboratory, Los Alamos, NM;
[b] University of California, San Diego, La Jolla, CA

ABSTRACT

This paper overviews the test setup and experimental methods for structural health monitoring (SHM) of two 9-meter CX-100 wind turbine blades that underwent fatigue loading at the National Renewable Energy Laboratory's (NREL) National Wind Technology Center (NWTC). The first blade was a pristine blade, which was manufactured to standard specifications for the CX-100 design. The second blade was manufactured for the University of Massachusetts, Lowell with intentional simulated defects within the fabric layup. Each blade was instrumented with piezoelectric transducers, accelerometers, acoustic emission sensors, and foil strain gauges. The blades underwent harmonic excitation at their first natural frequency using the Universal Resonant Excitation (UREX) system at NREL. Blades were initially excited at 25% of their design load, and then with steadily increasing loads until each blade reached failure. Data from the sensors were collected between and during fatigue loading sessions. The data were measured over multi-scale frequency ranges using a variety of acquisition equipment, including off-the-shelf systems and specially designed hardware developed at Los Alamos National Laboratory (LANL). The hardware systems were evaluated for their aptness in data collection for effective application of SHM methods to the blades. The results of this assessment will inform the selection of acquisition hardware and sensor types to be deployed on a CX-100 flight test to be conducted in collaboration with Sandia National Laboratory at the U.S. Department of Agriculture's (USDA) Conservation and Production Research Laboratory (CPRL) in Bushland, Texas.

Keywords: wind turbine, structural health monitoring, fatigue test, CX-100

1. INTRODUCTION

1.1 Motivation

Wind turbines are becoming a larger source of renewable energy in the United States. The turbine manufacturers have been increasing the length of the turbine blades, often made of composite materials, to maximize power output. As a result of severe wind loadings and material level flaws in composite structures, blade failure has become a more common occurrence in the wind industry. Monitoring the structural health of the turbine blades is particularly important, because they account for 15-20% of the total turbine cost. Blade damage is among the most expensive types of damage to repair, often requiring blade replacement, and it can cause serious secondary damage to the wind turbine system due to rotating imbalance created by blade failure. It is imperative that a structural health monitoring (SHM) system be incorporated into the design of the wind turbines in order to monitor flaws before they develop into catastrophic failure.

1.2 Overview

The authors have been investigating several design parameters of SHM techniques and the performance of high-frequency active-sensing SHM techniques, including wave propagation and diffuse wave-field transfer functions in time and frequency domains as a way to monitor the health of a wind turbine blade using piezoelectric sensors. In addition, a multi-scale sensing approach is proposed as a means to assess the influence of structural damage on the global dynamic response of a blade. In order to implement these systems in the field, compact sensor nodes, which the authors have been developing [1-3], are necessary. To that end, prototype embedded sensing hardware is tested alongside commercial-off-the-shelf (COTS) data acquisition systems. With the proposed sensing strategy, a series of full-scale fatigue tests were performed in collaboration with Sandia National laboratory (SNL) and the National Renewable Energy Laboratory (NREL). These tests are a precursor for a planned full-scale deployment of an SHM system on CX-100 rotor blades to be

*sgtaylor@lanl.gov

Figure 1. Test setup: a 9m CX-100 blade under a fixed-free condition

flown in collaboration with SNL at the U.S. Department of Agriculture's (USDA) Conservation and Production Research Laboratory (CPRL) in Bushland, Texas.

1.3 Test Structures

Two test structures were employed for fatigue testing. Each was a 9-m CX-100 blade [4], originally designed at Sandia National Laboratory. The first blade, dubbed the LANL blade, was manufactured according to standard specifications for the CX-100 blade. The LANL blade is shown mounted to the test fixture in Figure 1. The second blade, dubbed the University of Massachusetts, Lowell (UMass) blade, was manufactured with intentional defects. Each blade was mounted to a steel frame designed to approximate a fixed-free condition, and loads were introduced to the blade using a Universal Resonant EXcitation (UREX) system oscillating at the first resonant frequency of the blade.

2. LANL BLADE SENSOR ARRAYS

The LANL blade fatigue test was conducted primarily to provide model validation data for ongoing modeling efforts at LANL. Although other researchers independently installed sensors on the LANL blade, this section describes only those sensors installed and monitored by the authors. Several sensor arrays were installed on the blade, with most sensors concentrated near the root of the blade. With the exception of one microphone, all sensors were installed on the exterior of the blade. The primary sensor type employed was a 12mm diameter lead zirconate titanate (PZT) disk, although macro-fiber composite (MFC) patches and accelerometers, in addition to the microphone mentioned above, were employed as well. The PZT sensor arrays were predominantly arranged in a star configuration, for which sensing patches were located equidistant from a central actuating patch; an additional sensing patch was collocated with the actuator for some arrays. Some basic information for each sensor array is collected in Table 1. The array names given are based primarily on the data acquisition systems employing the respective sensor array, as described in Sec. 4. Detailed summaries of the sensor arrays are provided in the remainder of this section.

Table 1: LANL blade sensor array summary

Array Name	No. of Channels	Sensor Type	Configuration	Collocated Actuator/Sensor
WASP 1	6	PZT	Star	No
WASP 2	6	PZT	Star	No
Metis 1	7	PZT	Star	Yes
Metis 2	7	PZT	Star	Yes
Laser Inner	7	PZT	Star	No
Laser Outer	8	PZT	Star	Yes
NI Active	8	PZT	1D Linear	Yes
NI Passive	12	PZT, microphone, Accelerometer	2D Linear	N/A

2.1 Root Area

The low-pressure surface of the blade's root area contained active sensing arrays composed of PZT patches for WASP 1, Metis 1, as well as the LASER Inner and Outer arrays. A Diagram of the sensor arrays on the low-pressure surface of the blade's root area is shown in Figure 2. The inner array observes a 0.75 m diameter region centered 1m from the blade root, while the outer array observes a 2m elliptical region centered 1.5m from the root.

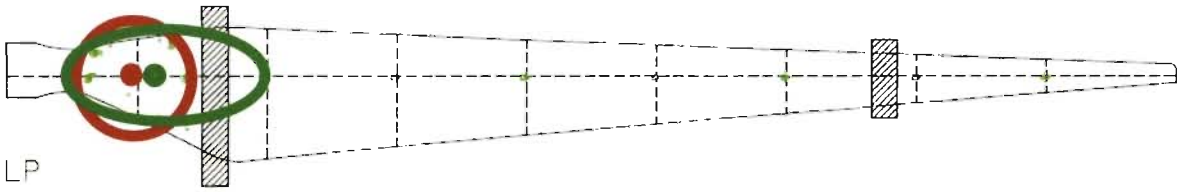

Figure 2. Sensor arrays installed in the root area on the low-pressure surface.

The high-pressure surface of the blade's root area contained active sensing arrays composed of PZT patches for WASP 2 and Metis 2. These two arrays were substantially identical, and each array relied on a centrally located actuator for excitation. The transmission distance ranged from 0.37m to 0.5m, and the actuating patches were located 1m from the blade root. A Diagram of the sensor arrays on the high-pressure surface of the blade's root area is shown in Figure 3.

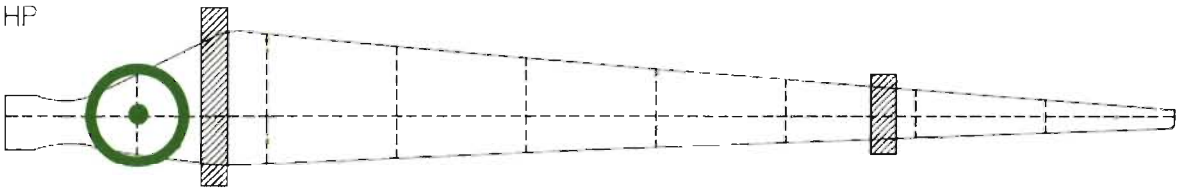

Figure 3. Sensor arrays installed in the root area on the high-pressure surface.

2.2 Aerodynamic Area

The low-pressure surface along the aerodynamic portion of the blade was instrumented with PZT patches, using collocated MFC patches as backup sensors. These sensors were positioned at one-meter increments along the blade, with an actuator located at the 5-meter station. A Diagram of the sensor arrays on the low-pressure surface along the blade's aerodynamic area is shown in Figure 4.

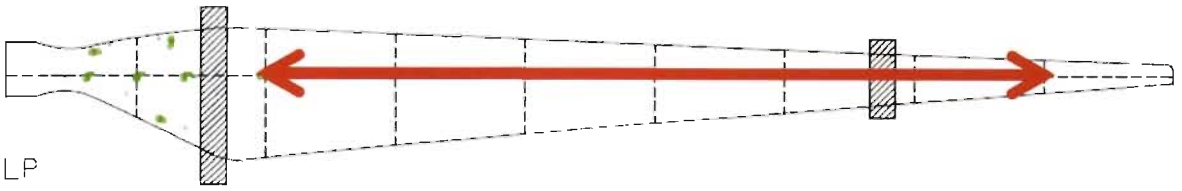

Figure 4. Sensor arrays installed along the aerodynamic area on the low-pressure surface.

The high-pressure surface along the aerodynamic portion of the blade was instrumented with seven accelerometer channels, three of which were part of a tri-axial sensor package. Of twelve passive measurement channels, five measured flapwise acceleration, one edgewise, and one lengthwise; an eighth channel was an audio microphone located inside the root of the blade; and four channels recorded PZT patches positioned to monitor strain along the spar cap. In addition to monitoring acceleration during the course of fatigue loading, the accelerometers (and in some tests, the PZT patches) were employed for modal testing of the blade. A Diagram of the sensor arrays on the high-pressure surface along the blade's aerodynamic area is shown in Figure 5.

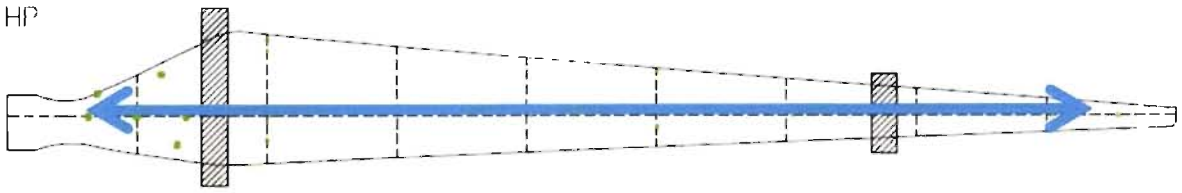

Figure 5. Sensor arrays installed along the aerodynamic area on the high-pressure surface.

3. UMASS BLADE SENSOR ARRAYS

The UMass blade was prepared primarily for digital image correlation (DIC) techniques [5] being implemented by researchers at UMass. Although other researchers installed sensors on the UMass blade, this section describes only the sensor arrays installed and interrogated by the authors. The LANL sensor layout for the UMass blade was less extensive than that for the LANL blade. Only one star-configuration array was installed to interrogate the root area; other arrays were positioned to observe the intentional defects in the blade, which were located in the aerodynamic portion. Further information concerning the defects will be described in future works. Because DIC techniques require an undisrupted image pattern to be visible on the surface of the blade, some of LANL's sensors were located inside the UMass blade rather than on its surface. Some basic information for each sensor array is collected in Table 1, and detailed summaries are provided in the remainder of this section.

Table 2: UMass blade sensor array summary

Array Name	No. of Channels	Sensor Type	Configuration	Collocated Actuator/Sensor
WASP Outboard	6	PZT	2D Linear	No
Metis Interior 1	5	MFC	2D Linear	No
Metis Interior 2	4	MFC	2D Linear	No
LASER Inboard	7	PZT	Star	Yes
LASER Outboard	8	PZT	2D Linear	Yes
Passive UMass	7	Accelerometer	2D Linear	N/A

3.1 Root Area

The low-pressure side of the UMass blade's root area was instrumented with one active sensing array using PZT patches. Each sensing patch was located a distance of 37.5 cm from the actuator patch, with the exception of one sensing patch collocated with the actuator. This array observes a region of the blade that has typically contained fatigue crack failures in the absence of blade defects. This array was laid out almost identically to the LASER Inner array on the LANL blade, which is depicted in Figure 2.

3.2 Aerodynamic Area

The low-pressure surface of the UMass blade's aerodynamic area was instrumented with two arrays in a two-dimensional linear configuration, which is depicted in Figure 6. The two arrays, the LASER Outboard and the WASP Outboard, were substantially similar to each other. These arrays were positioned to interrogate across two regions with known defects.

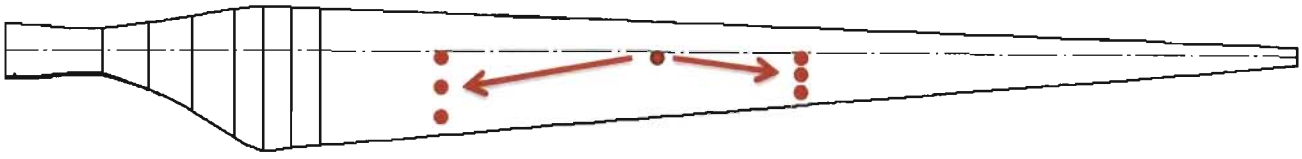

Figure 6. Sensor arrays installed along the UMass blade's aerodynamic area on the low-pressure surface.

The high-pressure surface of the UMass blade was instrumented with accelerometers in a similar configuration to that for the LANL blade, which is depicted in Figure 5. These sensors are intended to capture the global response of the blade as it undergoes fatigue loading, and provide feedback for model validation purposes.

The interior of the UMass blade's aerodynamic portion also housed several MFC patches, arranged in two separate 2D arrays. The configuration of the patches is depicted in Figure 7. These arrays directly straddle a known defect in the UMass blade, and are positioned to implement wave propagation methods across that defect.

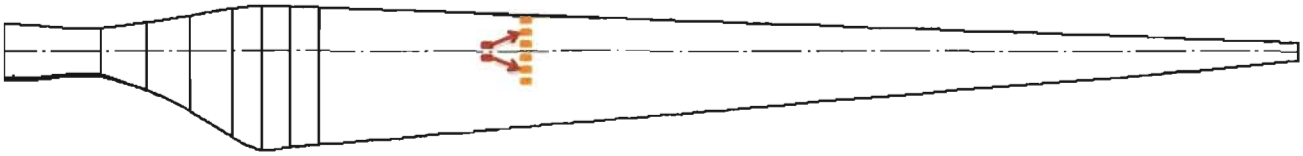

Figure 7. Sensor arrays in the interior of the UMass blade's aerodynamic portion.

4. EXPERIMENTAL METHODS AND EQUIPMENT

4.1 Modal Testing

Several modal tests were conducted on the LANL blade to provide a baseline characterization of the blade and to observe any changes to the blade's global behavior as the test progressed. A roving hammer test method was used, employing three shear accelerometers (PCB 352C22), four piezoelectric transducers (APC, 12mm diameter), and a modal impact hammer (PCB 086D20). The impact hammer tip was selected to excite frequencies up to 150Hz, which contains the first several modes. The blade was impacted at several points along the length and chord of the blade in both the flap-wise and edge-wise direction. A time record 4096 points was measured with a sampling frequency of 320 Hz. Five averages were taken for frequency response estimation, and no window was used.

A Bruel & Kjaer LASER data acquisition system was employed for the dual purpose of active sensing (see Sec. 4.2) and modal testing. Preliminary modal test results for this blade are shown in Table 1. These results are in agreement with previous modal surveys conducted on the CX-100 blade [6, 7]. The results will be used for model validation studies, which are being performed by the authors' research team. The first several fundamental modes of the blade were also compared to those measured by piezoelectric transducers. This test was intended to demonstrate the use of PZT sensors for multiple purposes: they can be used to detect the onset and monitor the growth of structural damage in the blade using higher frequency excitation, but they can also be used to identify lower-order global modes and assess the effect of structural damage. The piezoelectric transducers identified the resonant frequencies of a structure with the same accuracy provided by an accelerometer. After the initial modal testing, two saddles, which are visible in Figure 1, were added to the structure to increase the fatigue load and balance the moment distribution in the blade. This change in the structural condition significantly modifies the resonant frequencies as shown in Table 3.

Table 3: Modal Results for CX-100 Rotor Blade with the fixed-free Boundary Condition

Mode	Frequency (Hz) – before adding weights	Frequency (Hz) – after adding weights	Description
1	4.35	1.82	1st Flap Bending
2	6.43	2.68	1st Lag Bending
3	11.51	9.23	2nd Flap Bending
4	20.54	12.72	3rd Flap Bending
5	23.11	14.68	2nd Lag Bending
6	35.33	18.86	4th Flap Bending
7	46.27		1st Torsion
8	48.64	24.43	3rd Lag Bending

4.2 Diffuse Wave-Field Transfer Functions

Overview and frequency domain approach

Diffuse wave-field transfer functions can be used to monitor local regions of a structure for changes in the structure's behavior. Damage will alter the stiffness, mass, or energy dissipation properties of a system, which, in turn, results in the changes in system's local transfer functions. By utilizing piezoelectric active-sensors, a transfer functions can be measured in the range of tens or hundreds of kHz, which allows the method to be sensitive to small defects in the structure while remaining unaffected by low-frequency operational condition changes [8]. This method has been

demonstrated in our previous studies [9], where simulated damaged conditions were imposed. In our previous study, this method showed an intriguing ability to localize and detect damage when it was located anywhere along the spar of the blade section. This result is significant because the majority of the delamination in turbine blades occurs when the skin detaches from the spar.

A Bruel & Kjaer LASER data acquisition system was employed for the dual purpose of active sensing and modal testing. In the active sensing mode, the LASER system actively interrogated the CX-100 blade with band-limited white nose from 500 Hz to 40 kHz. Its utility in damage detection methods was demonstrated using simulated damage in the laboratory. For both the LANL and UMass blades, a switchbox was employed in order to utilize two sensor arrays: the LASER Inner and Outer arrays on the LANL blade; and the LASER Inboard and Outboard arrays on the UMass blade. The FRFs obtained from the blade were continuously updated for use as baselines against which to compare data collected at later testing intervals. The correlation coefficient or root mean squared deviation (RMSD) between the current baseline and new test data were used as a feature to track the progression of structural change over the course of the fatigue test.

The Wireless Active Sensing Platform (WASP) developed by the authors is a prototype embedded sensor node deployed in order to assess its performance in comparison to commercial systems such as the LASER. Because the WASP's firmware was still in development at the start of the test, it was limited to a 50 kHz sampling rate. On the LANL blade, the WASP interrogated an array substantially similar to the LASER Inner array, while on the UMass blade, it interrogated an array substantially similar to the LASER Outboard array. Although the WASP was designed for multi-path active sensing, it was limited in these tests to a single, dedicated excitation channel so that an external amplifier could be utilized to ensure a high signal-to-noise ratio.

Times domain approach

Time series predictive models, such as an autoregressive model with exogenous inputs (ARX), are also used as a damage-sensitive feature extractor. An ARX(p,q) model is fit to the data to capture the input/output relationship, which is intended to enhance the damage detection process by utilizing the information associated with a known input provided by a piezoelectric active-sensing system. In SHM, time series predictive models can be used as a damage-sensitive feature extractor using several approaches, including: (i) residual errors and (ii) ARX parameters. Standard multivariate classifiers can be used to distinguish between the sets of model parameters corresponding to the undamaged and damage classes. The time series analysis is the simplest of the techniques investigated and thus the memory and power usage of the system is minimal. This is ideal for a SHM system that needs to be self-powered when in operation on a real structure.

Two National Instruments (NI) 4431 module were employed for an 8-patch active sensing array. The NI 4431 modules have active sensing capabilities up to 51.2kHz using either PZT or MFC transducers. On the LANL blade, this system interrogated the NI Active array, but it was not employed for the UMass blade. The excitation provided was band-limited white noise ranging up to 50 kHz, with a sampling frequency of 100 kHz. Tests were conducted primarily while the blade was under dynamic load, with baseline measurements taken both while the blade was at rest and during the initial run-in of the blade.

4.3 Wave Propagation Methods

Lamb waves are mechanical waves corresponding to vibration modes of plates with a thickness on the same order of magnitude as the wavelength. The changes in wave attenuation, reflection, or time-of-flight are typically used to detect and locate damage. Various signal processing methods have been proposed to enhance the interpretation of the measured Lamb wave signals to detect and locate structural damage. These methods, which are based on changes in wave attenuation using wavelets, time-frequency analysis, wave reflections and scattering, and time-of-flight information, are well summarized in [10]. For isotropic materials, Lamb waves are defined specifically in terms of the wavelength of the transmitted wave and the material thickness in order to achieve optimal wave propagation. However, as a result of difficulties in selecting the optimal frequency for the fiberglass material in the CX-100 blade, several frequencies were used, as described next.

The MD7 IntelliConnector, by Metis Design, was employed for Lamb wave propagation over a range of transmission frequencies from 50kHz to 250kHz at 25kHz intervals, and at a sampling frequency of 10 MHz. On the LANL blade, the IntelliConnectors interrogated two star-type arrays, the Metis 1 and Metis 2, described in Table 1. This configuration allowed the IntelliConnectors to concentrate on the typical failure area for CX-100 blades. On the UMass blade, the

IntelliConnectors interrogated two neighboring 2D linear arrays of MFC patches, the Metis Interior 1 and 2 arrays, which are listed in Table 2. These patches were positioned directly across a known defect in anticipation of detecting early signs of fatigue cracking.

4.4 Passive Sensing

The aforementioned active-sensing methods can be utilized for damage detection of localized sensing areas, and they are less sensitive to operational variations than traditional sensors. However, a unique part of our proposed approach is the dual use of piezoelectric sensors (i.e. multi-scale sensing) for measuring global system response. The sensors can detect and locate structural damage using high frequency structural excitation/sensing, but the same sensor can be used to monitor low-frequency response changes, which allows one to estimate the effect of damage on system-level performance. In the course of the LANL blade fatigue test, several piezoelectric sensors were employed along the blade in order to measure its dynamic response during fatigue loading. These piezoelectric sensors were also co-located with accelerometers in order to compare their performance in low-frequency sensing. It is expected that, as the fatigue damage initiates and progresses, there will be meaningful changes in the low-frequency response signals. It should be noted that several of these passive sensors are also utilized as active-sensors for exciting and measuring the blade responses at high frequency ranges.

A National Instruments cRIO chassis was employed for passive sensing at a sampling rate of 1.6kHz. On the LANL blade, this system recorded measurements from accelerometers, PZTs, and a microphone mounted inside the root of the blade. On the UMass blade, the microphone channel was omitted.

4.5 Sensor Diagnostics

The sensor diagnostic process is one of the most important SHM components as, if there is a response change, one must be able to distinguish whether the change is caused by structural damage or simply by sensor failure. This is especially important for our test as more than eight million fatigue load cycles were applied to the LANL blade, and more than two million are expected to be applied to the UMass blade. Such loads can adversely affect the installation condition and functionality of piezoelectric transducers. The basis of the sensor diagnostic method employed is to track the capacitive nature of the PZT transducers, which manifests in the imaginary part of the measured electrical admittance. Physical degradation or breakage of a PZT transducer, or changes and the bonding condition between the transducer and its host structure can be identified using this method [11]. This sensor diagnostic method is implemented for this test with an efficient signal processing tool [12] that is not affected by uniformly varying temperature fluctuations or other operational condition changes.

A Hewlett Packard HP4291A was utilized to collect impedance measurements of all PZT patches at regular intervals throughout the course of the test. Each impedance measurement was taken using a frequency sweep from near DC to 30 kHz. The imaginary portion of the admittance curve was then utilized to infer the sensor bond condition. Regular and frequent sensor diagnostic checks were performed for the LANL blade, but they were not performed for the UMass blade.

5. SUMMARY

We have described the sensor type, purpose and layout for sensor arrays on two CX-100 blades that in 2011 and 2012 underwent fatigue loading until failure at NREL's NWTC. The LANL blade was manufactured according to standard specifications, while the UMass blade was manufactured with known, intentional defects. Several sensing systems were employed to interrogate the various sensor arrays, and some preliminary or baseline results have been presented. The analysis of the recorded data through the course of each test, including the application of SHM techniques relevant to the failure of each blade, are presented in our concurrent work [13].

ACKNOWLEDGEMENTS

This research was funded through the Laboratory Directed Research and Development program at Los Alamos National Laboratory. The authors would like to acknowledge Scott Hughes and Mike Desmond from National Renewable Energy Laboratory and Mark Rumsey and Jon White from Sandia National Laboratory for their support and guidance on this study.

REFERENCES

[1] S. G. Taylor, K. M. Farinholt, E. B. Flynn *et al.*, "A mobile-agent-based wireless sensing network for structural monitoring applications," Measurement Science and Technology(4), 045201 (2009).

[2] S. Taylor, K. Farinholt, G. Park *et al.*, "Multi-scale wireless sensor node for health monitoring of civil infrastructure and mechanical systems," Smart Structures and Systems, 6(5-6), 661-673 (2010).

[3] S. G. Taylor, J. Carroll, K. M. Farinholt *et al.*, [Embedded processing for SHM with integrated software control of a wireless impedance device] SPIE, San Diego, CA, USA(2011).

[4] D. Berry, "Design of 9-Meter Carbon-Fiberglass Prototype Blades: CX-100 and TX-100," SAND2007-0201, Sandia National Laboratories, Albuquerque, NM, (2007).

[5] M. N. Helfrick, C. Niezrecki, P. Avitabile *et al.*, "3D digital image correlation methods for full-field vibration measurement," Mechanical Systems and Signal Processing, 25(3), 917-927 (2011).

[6] D. T. Griffith, and T. G. Carne, [Experimental Modal Analysis of 9-meter Research-sized Wind Turbine Blades] Springer New York, (2011).

[7] K. Deines, T. Marinone, R. Schultz *et al.*, [Modal Analysis and SHM Investigation of CX-100 Wind Turbine Blade] Springer New York, (2011).

[8] G. Park, A. C. Rutherford, J. R. Wait *et al.*, "High-frequency response functions for composite plate monitoring with ultrasonic validation," AIAA journal, 43(11), 2431-2437 (2005).

[9] G. Park, S. G. Taylor, M. F. Kevin *et al.*, "SHM of Wind Turbine Blades Using Piezoelectric Active-Sensors." 321-326 (2010).

[10] A. Raghavan, and C. E. S. Cesnik, "Review of guided-wave structural health monitoring," Shock and Vibration Digest, 39(2), 91-116 (2007).

[11] G. Park, and D. J. Inman, "Structural health monitoring using piezoelectric impedance measurements," Philosophical Transactions A: Mathematical, Physical and Engineering Sciences, 365(1851), 373-392 (2007).

[12] T. G. Overly, P. Gyuhae, K. M. Farinholt *et al.*, "Piezoelectric Active-Sensor Diagnostics and Validation Using Instantaneous Baseline Data," Sensors Journal, IEEE, 9(11), 1414-1421 (2009).

[13] S. G. Taylor, H. Jeong, J. K. Jang *et al.*, [Full-scale fatigue tests of CX-100 wind turbine blades. Part II – analysis] SPIE, San Diego, CA(2012).